

Seasonal solar wind speeds for the last 100 years: Unique coronal hole structures during the peak and demise of the Grand Modern Maximum

K. Mursula¹, L. Holappa¹ and R. Lukianova^{2,3}

arXiv:1612.04941v1 [physics.space-ph] 15 Dec 2016

¹ReSoLVE Centre of Excellence, Space
Physics Research Unit, University of Oulu,
Oulu, Finland

²Geophysical Center of Russian Academy
of Science, Moscow, Russia

³Space Research Institute of RAS,
Moscow, Russia

Solar coronal holes are sources of high-speed solar wind streams, which cause persistent geomagnetic activity especially at high latitudes. Here we estimate seasonal solar wind speeds at 1 AU for the last 100 years using high-latitude geomagnetic measurements and show that they give information on the long-term evolution of important structures of the solar large-scale magnetic field, such as persistent coronal holes. We find that the centennial evolution of solar wind speed at 1 AU is different for equinoxes and solstices, reflecting differences in the evolution of polar coronal hole extensions and isolated low-latitude coronal holes. Equinoctial solar wind speeds had their centennial maximum in 1952, during the declining phase of solar cycle 18, verifying that polar coronal holes had exceptionally persistent extensions just before the peak of the Grand Modern Maximum of solar activity. On the other hand, solstice speeds had their centennial maximum during the declining phase of solar cycle 23 due to large low-latitude coronal holes. A similar configuration of seasonal speeds as in cycle 23 was not found earlier, not even during the less active cycles of early 20th century. Therefore the exceptional occurrence of persistent, isolated low-latitude coronal holes in cycle 23 is not related to the absolute level of sunspot activity but, most likely, to the demise of the Grand Modern Maximum.

1. Introduction

The large-scale evolution of solar wind (SW) and the interplanetary magnetic field is determined by the solar magnetic field, whose structure varies over the solar cycle [Wang *et al.*, 1991; McComas *et al.*, 2008; Pinto *et al.*, 2011]. The highest values of solar wind speed (V) at the Earth's orbit are observed during the declining phase of the solar cycle, when high-speed streams (HSS) from the equatorward extensions of polar coronal holes extend to low heliographic latitudes [Krieger *et al.*, 1973; Gosling *et al.*, 1976]. During their passage through the interplanetary space, HSS compress the ambient slow solar wind plasma and the interplanetary magnetic field, which may lead to the formation of corotating interaction regions (CIR). Coronal mass ejections and CIR/HSS hitting the Earth's magnetic field are the main drivers of geomagnetic activity. While coronal mass ejections produce the majority of strong geomagnetic storms, CIR/HSS produce a large fraction of storms of minor to moderate intensity [Richardson *et al.*, 2006; Zhang *et al.*, 2007]. However, the combination of high solar wind speed and Alfvén waves embedded in HSS produce strong and persistent auroral activity [Tsurutani *et al.*, 2006]. The annual occurrence of substorms is also strongly modulated by the occurrence of HSS [Tanskanen *et al.*, 2005, 2011].

High-speed streams have the largest relative effect on geomagnetic activity at high latitudes [Finch *et al.*, 2008; Lukianova *et al.*, 2012; Holappa *et al.*, 2014a], and high-latitude geomagnetic activity has been exploited to find information about the historical occurrence of HSS. Mursula *et al.* [2015] used observations at two high-latitude magnetic stations (Godhavn/Qeqertarsuaq, and Sodankylä) to reconstruct the annual means of

solar wind speed proxies over the last 100 years, covering the special time interval of the Grand Modern Maximum of solar activity [*Solanki et al.*, 2000]. They found that a short period of typically 1-2 years of high values of annual SW speed occurred in the declining phase of each of the eight studied solar cycles (16–23). During the declining phase of cycle 18 in the early 1950s, high HSS activity continued exceptionally long, for three successive years, with the highest annual speed found in 1952. *Mursula et al.* [2015] noted that cycle 19, which marks the sunspot maximum of the Grand Modern Maximum, was most likely preceded by exceptionally strong polar fields produced by frequent surges of new flux leading to persistent extensions of polar coronal holes during the declining phase of the previous cycle. This relation verifies one of the two basic tenets of solar dynamo theory of the poloidal-to-toroidal field transition (so called Ω mechanism) [*Babcock*, 1961] for the period of the highest known solar activity.

While the annual averages of solar wind speed give important insight to the long-term evolution of solar magnetic fields and coronal holes, a study using higher time resolution is useful because the typical lifetime of coronal holes is several solar rotations but less than a year [*Harvey and Sheeley Jr* [1979]; *Mursula and Zieger*, 1996; 2001]. Because of the 7.2° annual variation of the Earth's heliographic latitude, HSS from polar coronal holes (or their extensions) reach the ecliptic plane more often close to equinoxes. On the other hand, isolated equatorial or low-latitude coronal holes would lead to a larger relative fraction of Earth-bound HSS close to solstices. Thus, the differences in the long-term evolution of HSS between the seasons corresponding to low vs. high heliographic latitudes can be used to study the occurrence and the approximate location of persistent

coronal holes. In this paper we study the long-term evolution of HSS at seasonal time resolution during the last 100 years (1914-2014). The paper is organized as follows. In Section 2 we introduce the solar wind speed proxy and study its relation to the measured solar wind speed. In Section 3 we derive the seasonal solar wind speeds in 1914-2014. Finally, we discuss the implications of our results for the evolution of solar magnetic fields and coronal holes and give our conclusions in Section 4.

2. Extracting SW speeds from high-latitude disturbances

In order to obtain a long-term proxy of the seasonal SW speed we use the horizontal magnetic field measurements at Sodankylä observatory (geographic: 67.37° latitude, 26.63° longitude; geomagnetic: 64° lat and 119° long), located near the equatorward boundary of the auroral oval. At Sodankylä, recordings of the Earth's magnetic field vector have been made since 1914 (interrupted only by the World War II in 1945), forming the longest series of high-latitude geomagnetic measurements.

The largest perturbations at Sodankylä occur in the horizontal (H) geomagnetic component due to the auroral electrojets. During the growth and expansion phases of magnetospheric substorms, the westward auroral electrojet intensifies and expands, and decays back to the quiet-time level during the recovery phase [Akasofu, 1964]. The strongest westward currents during substorms are due to the substorm current wedge located around the midnight sector [Clauer and McPherron, 1974]. It has been shown that the substorm-related disturbances in the midnight sector are indeed dominated by HSS [Tanskanen *et al.*, 2005], while HSS have a smaller relative effect at other local times [Finch *et al.*, 2008]. Therefore, in order to have the best possible proxy for the solar wind speed we

use the data from the 20-23 UT (all four hours included) time interval, corresponding to 22-01 local time at Sodankylä.

We use the geomagnetic disturbance parameter ΔH as a measure of westward auroral electrojet intensity. We define ΔH as follows. For each month we calculate the quiet-time level $H(q)$ as the average of four-hourly night-time (22-01 local time) H values during the five quietest days of the month. (The quietest days have been determined from the local K indices and are available at Sodankylä observatory web page). Then we calculate the monthly disturbance ΔH by subtracting the monthly average of night-time H values of all days from $H(q)$. (Since disturbances reduce the H-component, ΔH will always be positive.) Then we calculate the seasonal (three-month) averages of the monthly ΔH values for spring (Feb-Apr), summer (May-Jul), fall (Aug-Oct) and winter (Nov-Jan). (Here seasons are mainly ordered by the Earth's heliographic latitude).

We also use the hourly means of solar wind speed V in 1964-2014 from the OMNI data base (<http://omniweb.gsfc.nasa.gov/>). While there are practically no data gaps in the Sodankylä H values during the space age (only 11 hourly means missing since 1964), there are numerous data gaps in the OMNI data base especially during 1980s and early 1990s. Therefore, we calculate seasonal means using only those night hours when simultaneous measurements of both ΔH and V exist. In order to have sufficient statistics, we neglect those seasonal values where the data coverage remains smaller than 30%.

Figure 1a shows a scatter plot between the solstice (summer and winter seasons) and equinox (spring and fall) means of ΔH and the measured seasonal solar wind speed V in 1964-2014, together with the best-fit regression lines. Table 1 gives the regression pa-

rameters (slope, intercept), correlation coefficients and the corresponding p-values (using first-order autoregressive AR(1) noise model) for the two fits. One can see that V increases more steeply as a function of ΔH during solstices than during equinoxes. Thus, a fixed value of V produces a larger disturbance ΔH during equinoxes than solstices. On the other hand, intercepts are closely similar, indicating a similar quiet-time level. This difference is related to the well known semiannual variation of geomagnetic activity, which is mainly due to the equinoctial [*Cliver et al.*, 2000; *Lyatsky et al.*, 2001] and Russell-McPherron [*Russell and McPherron*, 1973] effects modulating the strength of solar wind-magnetosphere coupling. Figures 1b and 1c show the fit residuals $\delta = V(\text{measured}) - V(\text{predicted})$ as a function of ΔH for equinoxes and solstices, respectively. Correlations are highly significant in both seasons (slightly better in solstices) and no obvious outliers are seen. Moreover, the residuals lie symmetrically around zero for the whole range of ΔH , indicating a homoscedastic distribution of errors. Thus, the standard least squares fit performs well and can be reliably used to reconstruct seasonal proxies for the solar wind speed.

3. Seasonal SW speeds in 1914-2014

The above discussed seasonal regressions between ΔH and the measured SW speed in 1964-2014 can now be applied to reconstruct the seasonal SW speeds for the pre-satellite era since 1914. Figures 2a and 2b show the SW speed proxies in 1914-2014 for equinoxes and solstices, respectively, together with the measured seasonal solar wind speeds in 1964-2014. Here all available data (not only simultaneous data with the solar wind measurements) are used when calculating measured and estimated SW speeds. Ac-

cordingly, Figure 2 presents the SW speed proxies for the case of gapless measurement of SW speeds. This slightly increases the differences between the measured and estimated SW speeds during the common time interval 1964-2014. However, this is unavoidable and irrelevant for this paper where the main purpose is to compare the two seasonal SW speed proxies.

Figure 2 shows that there are some significant and interesting differences between the SW speed proxies for equinoxes and solstices. Low (< 400 km/s) seasonal means of solar wind speed occur more often during solstices than during equinoxes, which can be seen both in the measured and proxy values especially in recent decades (since 1990s). The highest equinox maxima occurred in 1952 and 1994 while the highest solstice maxima occurred in 1930 and 2003. Because of these differently timed maxima, the long-term evolution of solar wind speed is quite different during equinoxes and solstices. (Note also that SW speed was not particularly high around 1960, in the declining phase of the all-time high sunspot cycle 19, ahead of the low sunspot cycle 20).

The peaks in Figure 2 correspond to individual seasonal (three-monthly) means, thus reflecting a rather short-term occurrence of coronal holes. We also want to study the occurrence of the most persistent coronal hole structures lasting for longer than one season. For that, we show in Figure 3 the three-point running means of the seasonal SW speeds of Figure 2, separately for equinox and solstice proxies. Thus, each point in Figure 3 gives an average over 1.5 years. Figure 3 shows that some of the peaks in Figure 2, in particular the solstice peak in 1930 was based only on one high (summer) solstice value, and lost in relative height in Figure 3. Others, in particular the equinox peak in 1952 and the

solstice peak in 2003 correspond to the most persistent coronal hole activity and retain their all-time (centennial) high peak status during the respective season in Figure 3.

Figure 3 shows interesting similarities and differences in the long-term evolution of the reconstructed SW speed between equinoxes and solstices and, thereby, between polar coronal hole extensions and low-latitude coronal holes. During the low cycles 15 and 16, SW speeds attained roughly similar peak values of about 460-470 km/s in both seasons. During the next, more active cycle 17, the peak values remained still at a fairly similar level but both the solstice speed and especially the equinox speed depict 2-3 peaks of roughly equal height. The two curves are then separated in cycle 18, when the equinox speeds attain their all-time maximum value of about 520 km/s. Note that the solstice peak in cycle 18 and in most remaining cycles (19, 21, 22), as well as all equinox peaks since cycle 19 reach a roughly similar level of about 490-500 km/s, which is somewhat higher than the level of peaks during the low cycles 15-17. During cycle 20 the solstice peak remains at the low level of the early cycles. Interestingly, both speeds depict multiple peaks during cycle 22, just before the solstice speed reaches its all-time maximum in cycle 23. This evolution resembles the evolution of speeds during cycles 17-18 before the all-time peak in equinox speed. Note also that the two all-time maxima attain surprisingly similar values.

Figure 3 also shows that during solar minima the solar wind speed is systematically lower during solstices than equinoxes. This is expected because the Earth is within the slow solar wind of the streamer belt more often during solstices than during equinoxes. (This was seen also for the unsmoothed seasonal solar wind speeds in Figure 2.) Note also

that while the equinox and solstice minima are quite similar during the minima between cycles 14-15 and 15-16, the difference is significantly larger during the minima of the more active cycles. The level of equinox minima is considerably raised during the more active cycles, but also the solstice minima attains higher values. This indicates that the streamer belt was rather stable and wide during the minima of the low cycles, but thinner and probably also more tilted during the minima of more active cycles. (Note that larger activity tends to increase longitudinal asymmetry and, thereby, lead to a larger tilt).

The recent very deep minimum in 2009 can be seen both in solstice and equinox speeds. During this minimum all equatorial and low-latitude coronal holes (and polar coronal hole extensions) disappeared [Tsurutani *et al.*, 2011], leading to the slowest solar wind speed during the space age. Interestingly, Figure 3 shows that the level of persistent solar wind speeds during this minimum is almost exactly the same as during the first two minima, indicating a return of the coronal and solar wind speed conditions to a similar situation as 100 years ago.

4. Discussion and Conclusions

In this paper we have used the longest available set of high-latitude geomagnetic observations to reconstruct a local measure (ΔH) of geomagnetic disturbance level which is suitable to study the long-term evolution of Earth-bound solar wind speed. We have quantified the relation between ΔH and the measured solar wind speed separately during equinoxes and solstices, finding high correlations for both seasons. We have estimated the seasonal means of the solar wind speed in 1914-2014 separately for equinoxes and solstices. Even though the 7.2° inclination of the Earth's orbit with respect to the he-

liographic equator is rather small, it is large enough to depict long-term variations in the latitudinal distribution of coronal holes, especially, in the relative effective fraction of polar coronal hole extensions and isolated low-latitude coronal holes.

Interestingly, we find that the long-term evolution of solar wind speed is quite different during equinoxes and solstices. While the solar wind speed during equinoxes shows a centennial maximum in 1952, during the declining phase of cycle 18, the solstice speeds maximise in 2003, during the declining phase of cycle 23. These two years were also the highest peaks in annual solar wind speed proxies during the last 100 years [*Mursula et al.*, 2015]. We have found here that, with increasing sunspot activity since cycle 17, extensions of polar coronal holes (and thereby polar fields) increase rapidly, leading to the centennial maximum of equinoctial solar wind speed during cycle 18. We suggested earlier that the exceptionally high solar wind speed in 1952 reflects the persistent existence of equatorward extensions of polar coronal holes, signaling the build-up of strong polar magnetic fields during the declining phase of cycle 18 [*Mursula et al.*, 2015]. However, this explanation does not apply to the peak in 2003, since the polar fields remained rather weak during the declining phase of solar cycle 23 and the minimum thereafter [*Smith and Balogh*, 2008; *Wang et al.*, 2009].

We have shown here that the solar wind speed peak in 2003 was the centennial maximum during solstices (but not during equinoxes), indicating that the HSS observed at 1 AU in 2003 largely emanated from isolated low-latitude coronal holes rather than from polar coronal hole extensions. It is known that exceptionally persistent, isolated low-latitude coronal holes existed during the declining phase of cycle 23 [*Gibson et al.*, 2009; *Fujiki*

et al., 2016]. So, cycle 23 was unique in persistent low-latitude coronal hole activity during the last 100 years. Interestingly, no equally persistent low-latitude coronal holes are found during last 100 years, including the very low-active cycles in the beginning of the 20th century. One might expect that during such low cycles, when polar fields remain weak and polar coronal holes rather limited, low-latitude coronal holes and related Earth-bound high-speed streams could be more typical than during the more active cycles. However, this is not the case. Thus, the coronal hole evolution in cycle 23 was unique during the last 100 years, probably reflecting the demise of the Grand Modern Maximum. It is likely that this change in coronal holes is related to the other unique features of cycle 23, such as the exceptionally weak polar magnetic fields [*Smith and Balogh*, 2008] and the changes in the distribution of magnetic fields [*Penn and Livingston*, 2006] and sizes [*Lefèvre and Clette*, 2011; *Clette and Lefèvre*, 2012] of sunspots, and in their relation to several other solar parameters [*Lukianova and Mursula*, 2011]. Only later work will reveal if and how all these observed, unique features of cycle 23 are related to each other and to the corresponding changes in global solar magnetic fields.

While the solar wind speed minima of low-activity cycles attain quite similar, very low values in equinoxes and solstices, the minimum speeds of more active cycles are higher in both seasons. Moreover, the equinoctial speed minima increase faster than solstice speed minima when the overall solar activity increases. These results give strong evidence that the properties of the streamer belt also varied with long-term solar activity during the last 100 years.

Acknowledgments. We acknowledge the financial support by the Academy of Finland to the ReSoLVE Centre of Excellence (project no. 272157). We thank the Sodankylä Geophysical Observatory for providing the magnetic field data at (<http://www.sgo.fi/>). The solar wind data were downloaded from the OMNI2 database (<http://omniweb.gsfc.nasa.gov/>).

References

- Akasofu, S.-I., The development of the auroral substorm, *Planet. Space Sci.*, *12*, 273–282, 1964.
- Babcock, H. W., The topology of the Sun’s magnetic field and the 22-year cycle, *Astrophys. J.*, *133*, 572–587, 1961.
- Clauer, C. R., and R. L. McPherron, Variability of mid-latitude magnetic parameters used to characterize magnetospheric substorms, *J. Geophys. Res.*, *79*(19), 2898–2900, doi:10.1029/JA079i019p02898, 1974.
- Clette, F., and L. Lefèvre, Are the sunspots really vanishing?-anomalies in solar cycle 23 and implications for long-term models and proxies, *J. Space Weather Space Clim.*, *2*, A06, 2012.
- Cliver, E. W., Y. Kamide, and A. G. Ling, Mountains versus valleys: Semiannual variation of geomagnetic activity, *J. Geophys. Res.*, *105*, 2413–2424, doi:10.1029/1999JA900439, 2000.
- Finch, I. D., M. L. Lockwood, and A. P. Rouillard, Effects of solar wind magnetosphere coupling recorded at different geomagnetic latitudes: Separation of directly-driven and storage/release systems, *Geophys. Res. Lett.*, *35*, L21105, doi:10.1029/2008GL035399,

2008.

Fujiki, K., M. Tokumaru, K. Hayashi, D. Satonaka, and K. Hakamada, Long-term trend of solar coronal hole distribution from 1975 to 2014, *The Astrophysical Journal Letters*, *827*(2), L41, 2016.

Gibson, S. E., J. U. Kozyra, G. de Toma, B. A. Emery, T. Onsager, and B. J. Thompson, If the Sun is so quiet, why is the Earth ringing? A comparison of two solar minimum intervals, *J. Geophys. Res.*, *114*(A13), A09105, doi:10.1029/2009JA014342, 2009.

Gosling, J. T., J. R. Asbridge, S. J. Bame, and W. C. Feldman, Solar wind speed variations: 1962-1974, *J. Geophys. Res.*, *81*, 5061–5070, 1976.

Harvey, J. W., and N. R. Sheeley Jr, Coronal holes and solar magnetic fields, *Space Sci. Rev.*, *23*(2), 139–158, 1979.

Holappa, L., K. Mursula, T. Asikainen, and I. G. Richardson, Annual fractions of high-speed streams from principal component analysis of local geomagnetic activity, *J. Geophys. Res.*, *119*(6), 4544–4555, doi:10.1002/2014JA019958, 2014a.

Krieger, A. S., A. F. Timothy, and E. C. Roelof, A coronal hole and its identification as the source of a high velocity solar wind stream, *Sol. Phys.*, *29*, 505–525, 1973.

Lefèvre, L., and F. Clette, A global small sunspot deficit at the base of the index anomalies of solar cycle 23, *Astron. Astrophys.*, *536*, L11, 2011.

Lukianova, R., and K. Mursula, Changed relation between sunspot numbers, solar uv/euv radiation and tsi during the declining phase of solar cycle 23, *J. Atm. Sol.-Terr. Phys.*, *73*(2), 235–240, 2011.

- Lukianova, R., K. Mursula, and A. Kozlovsky, Response of the polar magnetic field intensity to the exceptionally high solar wind streams in 2003, *Geophysical Research Letters*, *39*(4), 2012.
- Lyatsky, W., P. T. Newell, and A. Hamza, Solar illumination as cause of the equinoctial preference for geomagnetic activity, *Geophys. Res. Lett.*, *28*, 2353–2356, doi:10.1029/2000GL012803, 2001.
- McComas, D. J., R. W. Ebert, H. A. Elliott, B. E. Goldstein, J. T. Gosling, N. A. Schwadron, and R. M. Skoug, Weaker solar wind from the polar coronal holes and the whole sun, *Geophys. Res. Lett.*, *35*(18), 2008.
- Mursula, K., and B. Zieger, The 13.5-day periodicity in the Sun, solar wind, and geomagnetic activity: The last three solar cycles, *J. Geophys. Res.*, *101*(A12), 27,077–27,090, 1996.
- Mursula, K., and B. Zieger, Long-term north-south asymmetry in solar wind speed inferred from geomagnetic activity: A new type of century-scale solar oscillation?, *Geophys. Res. Lett.*, *28*, 95–98, doi:10.1029/2000GL011880, 2001.
- Mursula, K., R. Lukianova, and L. Holappa, Occurrence of high-speed solar wind streams over the grand modern maximum, *Astrophys. J.*, *801*(1), 30, 2015.
- Penn, M. J., and W. Livingston, Temporal changes in sunspot umbral magnetic fields and temperatures, *Astrophys. J. Lett.*, *649*(1), L45, 2006.
- Pinto, R. F., A. S. Brun, L. Jouve, and R. Grappin, Coupling the solar dynamo and the corona: wind properties, mass, and momentum losses during an activity cycle, *Astrophys. J.*, *737*(2), 72, 2011.

- Richardson, I. G., et al., Major geomagnetic storms ($Dst \leq -100$ nT) generated by corotating interaction regions, *J. Geophys. Res.*, *111*, A07S09, doi:10.1029/2005JA011476, 2006.
- Russell, C. T., and R. L. McPherron, Semiannual variation of geomagnetic activity, *J. Geophys. Res.*, *78*(1), 92–108, 1973.
- Smith, E. J., and A. Balogh, Decrease in heliospheric magnetic flux in this solar minimum: Recent ulysses magnetic field observations, *Geophys. Res. Lett.*, *35*(22), 2008.
- Solanki, S. K., M. Schüssler, and M. Fligge, Evolution of the sun's large-scale magnetic field since the maunder minimum, *Nature*, *408*, 445–447, 2000.
- Tanskanen, E. I., J. A. Slavin, A. J. Tanskanen, A. Viljanen, T. I. Pulkkinen, H. E. J. Koskinen, A. Pulkkinen, and J. Eastwood, Magnetospheric substorms are strongly modulated by interplanetary high-speed streams, *Geophys. Res. Lett.*, *32*, L16104, doi:10.1029/2005GL023318, 2005.
- Tanskanen, E. I., T. I. Pulkkinen, A. Viljanen, K. Mursula, N. Partamies, and J. A. Slavin, From space weather toward space climate time scales: Substorm analysis from 1993 to 2008, *Journal of Geophysical Research (Space Physics)*, *116*(A15), A00I34, doi:10.1029/2010JA015788, 2011.
- Tsurutani, B., E. Echer, and W. Gonzalez, The solar and interplanetary causes of the recent minimum in geomagnetic activity (mga23): a combination of midlatitude small coronal holes, low imf bz variances, low solar wind speeds and low solar magnetic fields, *Ann. Geophys.*, *29*(5), 839, 2011.

Tsurutani, B. T., et al., Corotating solar wind streams and recurrent geomagnetic activity:

A review, *J. Geophys. Res.*, *111*, A07S01, doi:10.1029/2005JA011273, 2006.

Wang, Y.-M., N. R. Sheeley Jr., and A. Nash, A new solar cycle model including merid-

ional circulation, *Astrophys. J.*, *383*, 431–442, 1991.

Wang, Y.-M., E. Robbrecht, and N. R. J. Sheeley, On the weakening of the polar magnetic

fields during solar cycle 23, *Astrophys. J.*, *707*(2), 1372, 2009.

Zhang, J., et al., Solar and interplanetary sources of major geomagnetic storms (Dst <

-100 nT) during 1996-2005, *J. Geophys. Res.*, *112*, A10,102, doi:10.1029/2007JA012321,

2007.

	Equinoxes	Solstices
slope a [km/s/nT]	1.11	1.58
intercept b [km/s]	369	359
cc	0.74	0.80
p-value	$< 10^{-11}$	$< 10^{-8}$

Table 1. Regression parameters (slope a intercept b), correlation coefficients (cc) and p-values for equinoxes and solstices.

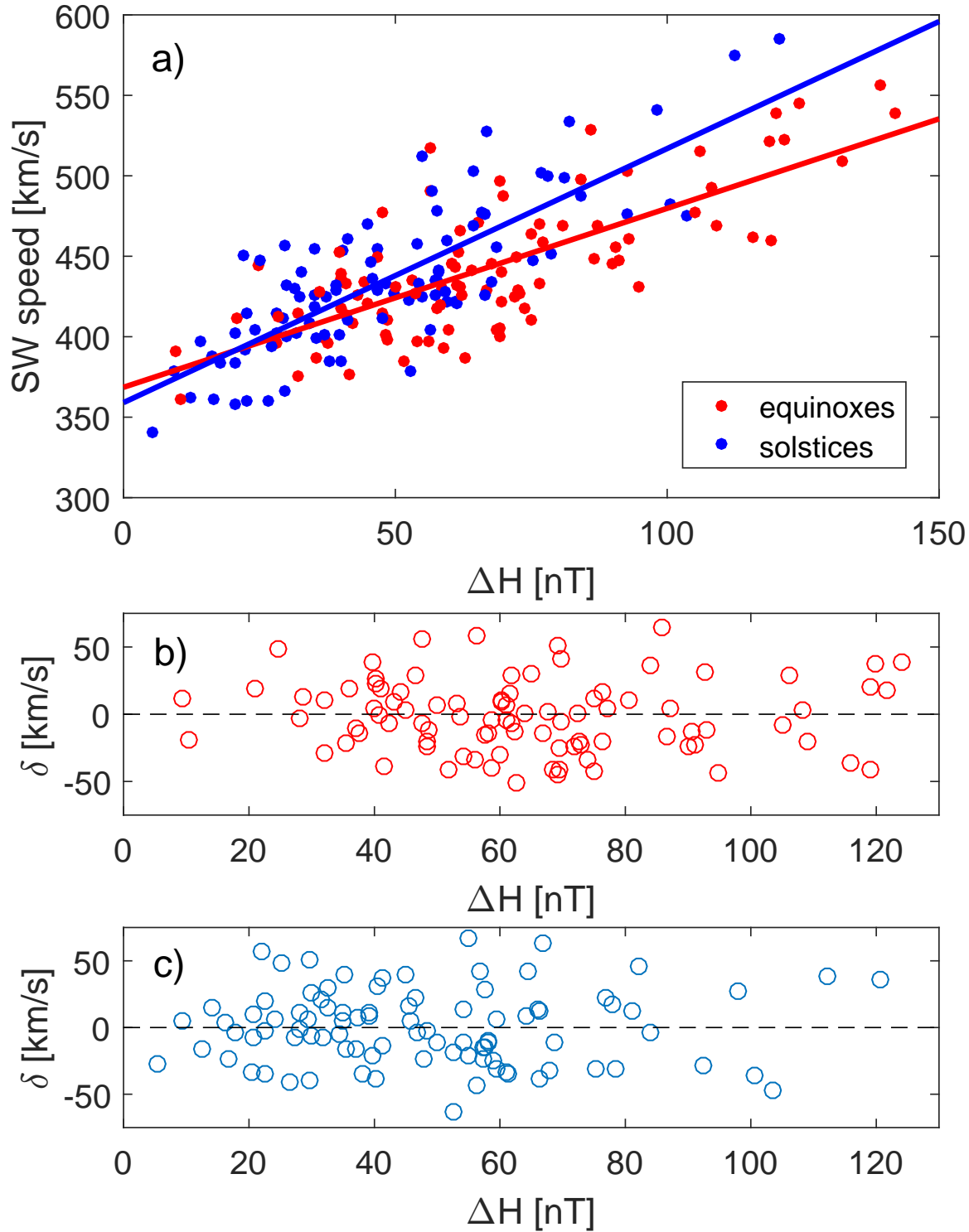


Figure 1. a) Scatter plot between seasonal means of ΔH and solar wind speed during equinoxes (red dots) and solstices (blue dots), together with their best-fit lines. b) Residuals of regressions as a function of ΔH for equinoxes and c) solstices.

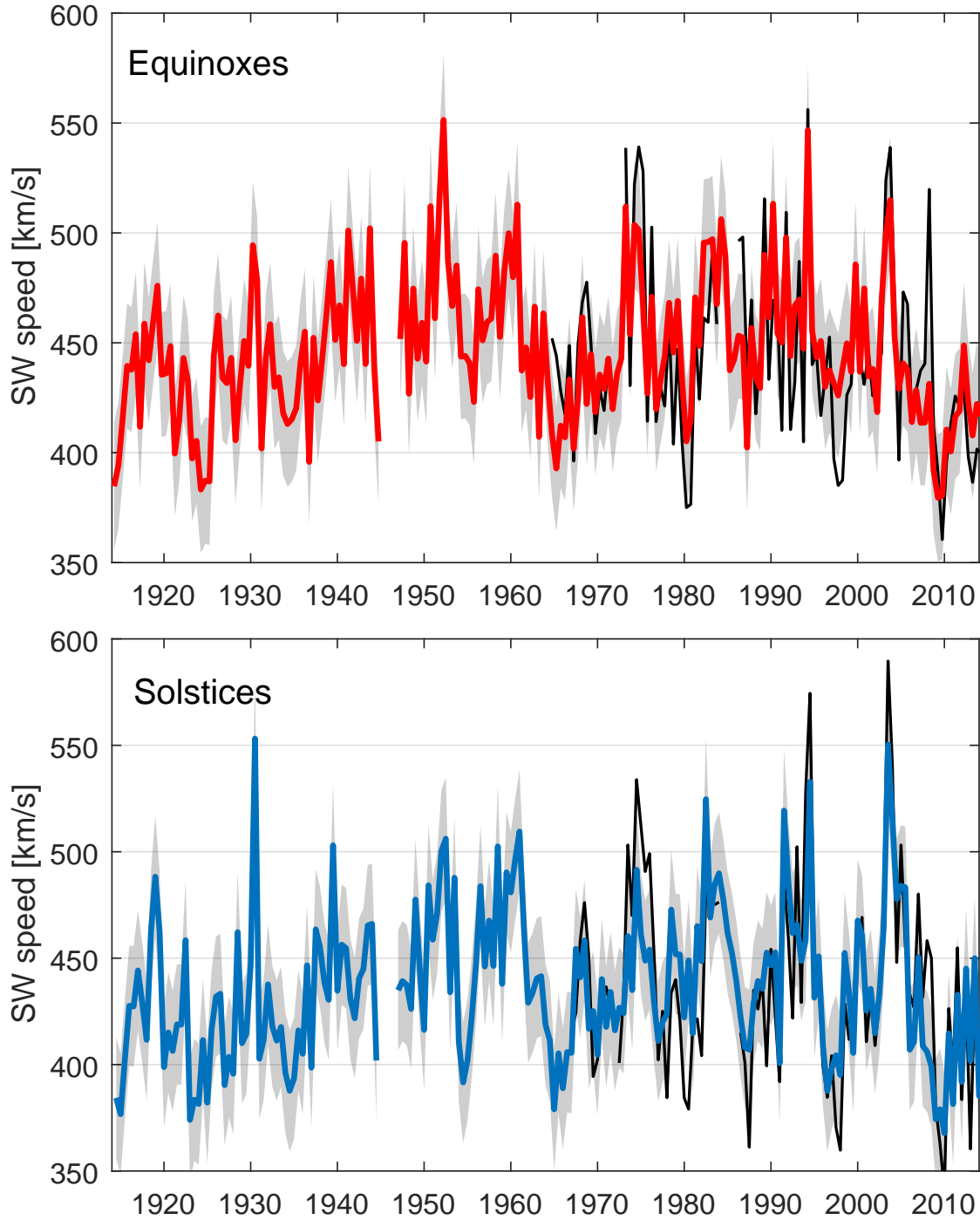


Figure 2. Solar wind speed proxies for a) equinoxes (red line) and b) solstices (blue line) with $\pm 1\sigma$ error estimates (shaded gray areas). Black lines denote the measured seasonal means of solar wind speed.

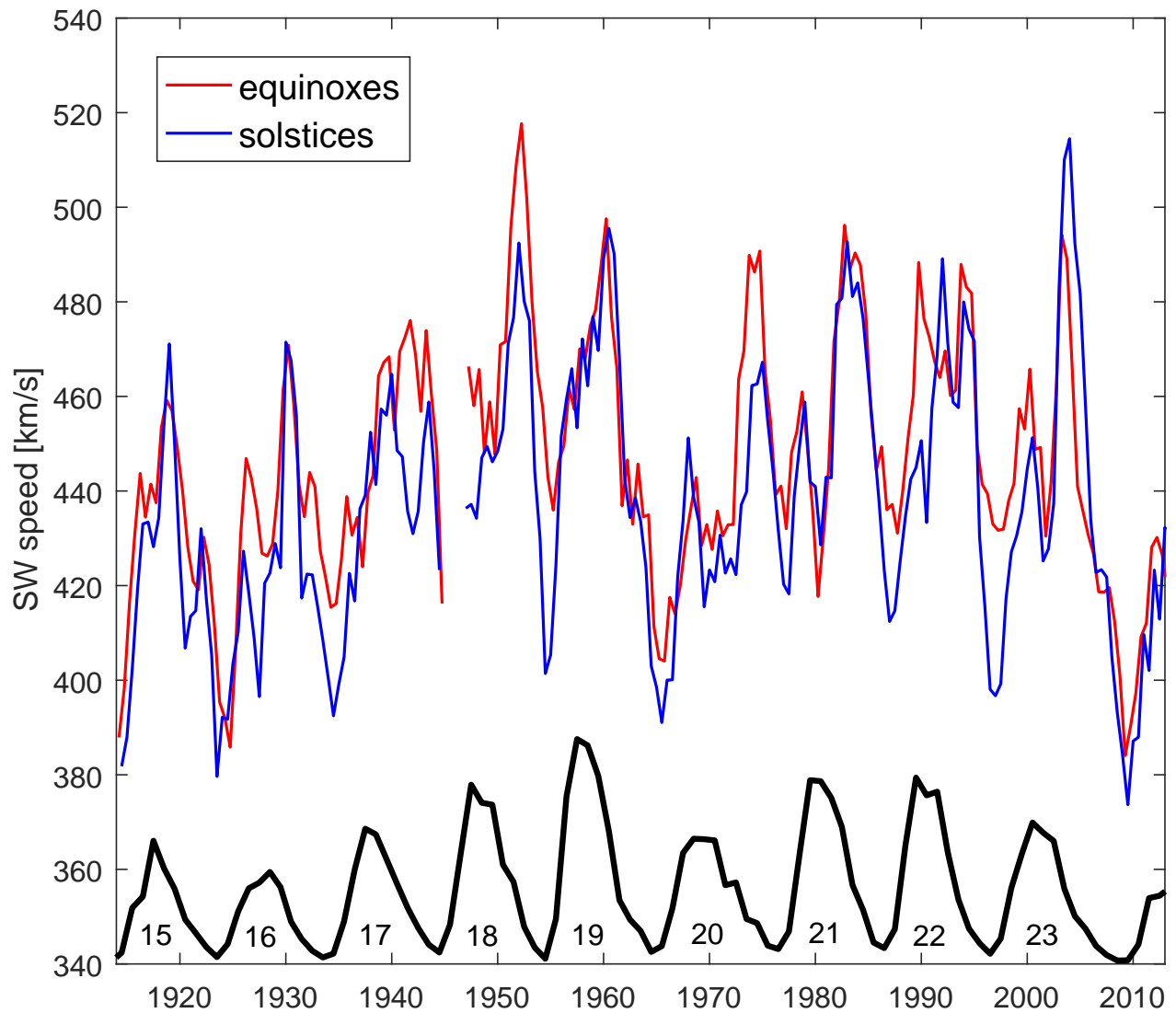


Figure 3. Three-point running means of the reconstructed solar winds speeds for equinoxes and solstices. Annual sunspot number (arbitrary scale) and solar cycle numbers are included for reference.